Journal of Physics: Conference Series **2687** (2024) 022032 doi:10.1088/1742-6596/2687/2/022032

Earthquake Measurements and Those Analysis on IR Components and Belle II Detector in KEK

H Yamaoka, M Masuzawa, T Kanayama, and M Maki

High Energy Accelerator Research Organization, 1-1 Oho, Tsukuba, Ibaraki, 3050801, Japan.
yamaokah@post.kek.jp

Abstract. Earthquakes frequently occur in Japan. Even though countermeasures are thoroughly considered and well executed, earthquakes still impact facilities and experimental devices. The large relative displacements induced by an earthquake can damage beam pipe bellows and interfere with sub-detectors by causing the tolerance between them to disappear. Even magnet quenches have been triggered by induced voltages caused by the relative displacements between the superconducting solenoids (i.e., the detector solenoid and the compensating solenoids surrounding the final focus quadrupole magnets, or QCSs). In response, we installed acceleration sensors on the Belle II detector and mounted gap sensors on the QCSs to measure the relative displacements. These measurements enabled the characteristics of the earthquakes that have affected the Belle II detector to be analysed. Response spectrum analyses (RSAs) of the Belle II detector were conducted to evaluate the impact of earthquakes according to the ground motion measurements. We then compared the measurements to the RSA results, which led to an idea for a countermeasure.

1. Introduction

The purpose of this study was to understand the cause of a power shutdown of the superconducting quadrupole magnets (QCSs) at the interaction region of the Belle II detector, which is located at the SuperKEKB accelerator complex at KEK (High Energy Accelerator Research Organization) in Tsukuba, Japan. A schematic showing its layout is shown in figure 1 [1, 2, 3].

The QCSs are supported in the cantilever by the accelerator tunnel. Hence, they have a support system independent of the Belle II detector. The power shutdown first occurred on March 20, 2021 during an earthquake with an intensity of 3.5 as per the Japan Meteorological Agency (JMA) scale.

At the interaction region of the Belle II detector, there is also a superconducting detector solenoid (that can produce a magnetic field of 1.5 T) and superconducting compensation solenoids that cancel the detector solenoid field at the QCS. The size of the Belle II detector is 8 × 8 × 10 m (length, width, and height, respectively) and its total weight is 1400 tons. An image of the detector is shown in Figure 2 [4].

The power shutdown of the QCSs was expected to be caused by disturbed magnetic fields in the solenoids, as the earthquake-induced voltage in the compensation solenoids exceeded the pre-set threshold (i.e., the QCS quench was triggered).

The second time the power shutdown occurred was on November 1, 2021, when another earthquake with an intensity of 3.5 occurred. This second event prompted an investigation into the cause of power shutdown. Because the cause of the power shutdown was assumed to be an induced voltage generated via disturbances in the magnetic field, the relative displacements between the Belle II detector and the QCSs were measured as an initial approach.

As part of this task, response spectrum analyses (RSA) were carried out for a 3D model of the Belle II detector to estimate the displacements in the detector via simulation. The RSA results showed that the Belle II detector can be shaken by up to a few mm by an earthquake with an intensity of 4 [5]. Because of the precision required by the detector and accelerator design, these displacements and interferences were taken seriously. In addition, if the displacement reached beyond the acceptable tolerance, it would be possible for damage to the beam pipe bellows connected to the QCSs to occur, and interference between the sub-detectors could also occur if the gaps between them disappeared.

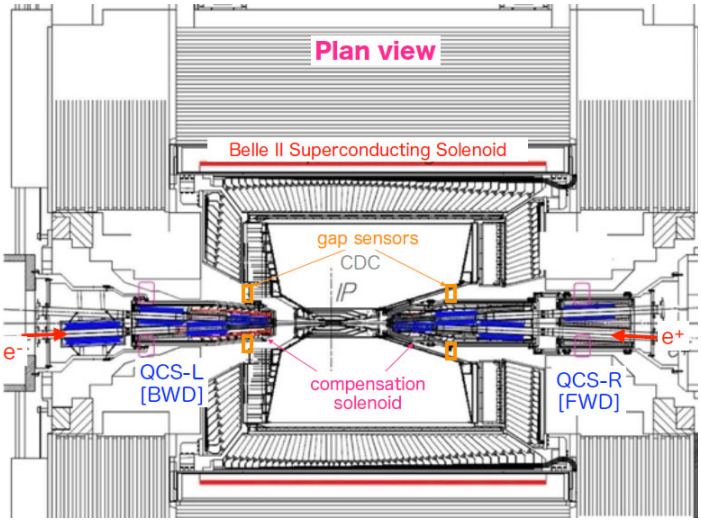

Figure 1. Schematic of the BelleII detector, showing the detector solenoid, final focus quadrupole magnets (QCSs), compensation solenoid, and gap sensors.

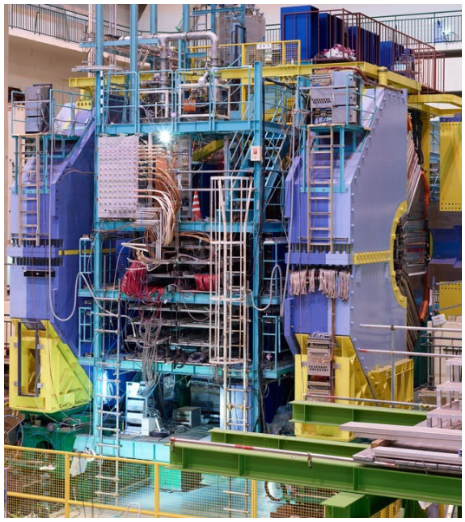

Figure 2. Image of the Belle II detector.

By installing acceleration sensors on the Belle II detector and the underground floor beneath it, these issues were investigated in more detail. Specifically, the following tasks were completed:

- Verification of the cause of the power shutdown.
- Verification of the RSA results.
- Measurement of the characteristics of seismic activity acting on the Belle II detector and the underground floor beneath it.
- Measurement of the relative displacement between the Belle II detector and the underground floor beneath it.

2. Measurement system

Two acceleration sensors were mounted on both the top of the Belle II detector (Belle II-top) and the underground floor 16 m below it (GL-16m), as shown in Figure 3. One sensor was a piezo-type tri-axial acceleration sensor (Acc-1), and its precision was 0.05 gal. The other was a servo-type high-precision acceleration sensor (Acc-2) with 10^{-6} gal precision.

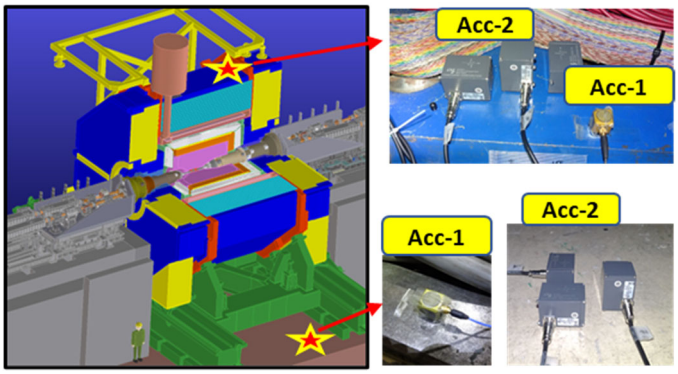

Figure 3. Earthquake measurement system.

These four sensors measured the seismic acceleration in three directions. The specifications of each sensor are shown in table 1. The piezo-type tri-axial acceleration sensors were installed at the end of May 2022, and the servo-type high-precision sensors were installed after the power to the Belle solenoid was temporarily turned off at the end of June 2022. The gap sensors mentioned in the next section were installed after the quench incidents (November 2021).

Table 1. Technical specifications of the sensors.

Name	Acc-1	Acc-2
Type	Piezo	Servo
Company	Imc	Tokkyo-kiki
Range	0.5 – 3 kHz	0.1 – 400 Hz
Sensitivity	1mV/gal	30.7mV/gal
Precision	0.05 gal	10^{-6} gal

The displacements were measured with the high-precision sensor (Acc-2) to obtain the cumulative sum (integration) of the acceleration histories, which were processed using a high-pass filter with a cut-off frequency of 0.5 Hz to remove the DC offset and trend. The integration error was estimated by, [6]

$$\Delta x < \frac{1}{(3ft)^{1/2}} t^2 \Delta a$$

where Δx is the integration error, t is the sampling time, Δa is the acceleration error, and f is the sampling frequency. In this study, the value of these parameters was t = 60 s, $\Delta a = 10^{-6}$ gal, and f = 256 Hz. Thus, the integration error was 1.7×10^{-4} mm, which was negligible compared to the displacement measurements. The earthquake data were measured automatically when a trigger level of 5 gal was reached.

3. Verification of the cause of the power shutdown

The cause of the QCS power shutdown was verified using the gap sensors, which were attached to the forward (FWD) QCS-R cryostat and backward (BWD) QCS-L cryostat. The precision of the gap sensors was 0.6 μm, and they measured the gaps between the QCS cryostats and the inner wall of the central drift chamber (CDC) in the lateral (NS) and vertical (UD) directions (i.e., in the plane perpendicular to the beam axis).

Table 2. Maximum gap displacement between the QCS's and the CDC in the lateral (NS) direction. Values in parentheses are estimated ones for an earthquake intensity of 3.5 assuming the displacement is proportional to $10^{(3.5\text{-}I)/2}$ [7].

Date	Intensity(I)	FWD (mm)	BWD (mm)	Difference(mm)
May 3	1.3(3.5)	0.0359(0.45)	0.0364(0.46)	0.0005(0.006)
May 5	2.4(3.5)	0.099(0.35)	0.104(0.37)	0.0053(0.019)
May 8	0.8(3.5)	0.0189(0.42)	0.0194(0.43)	0.0005(0.011
May 9	1.0(3.5)	0.0371(0.66)	0.0353(0.63)	0.0017(0.030)
May 22	2.4(3.5)	0.091(0.32)	0.083(0.29)	0.0084(0.030)

Table 2 lists the maximum gap displacements for the earthquakes occurred in May, 2022. Examples of the displacement histories measured by the gap sensors are shown in figure 4, which display the data collected on May 22, 2022. Figure 5 shows the Fourier amplitudes as a function of frequency for the earthquake that occurred on May 5, 2022. The natural frequencies of the Belle II detector, QCS-L (BWD), and QCS-R (FWD) are represented by the prominent peaks at 4.2 Hz, 23 Hz, and 13.8 Hz, respectively.

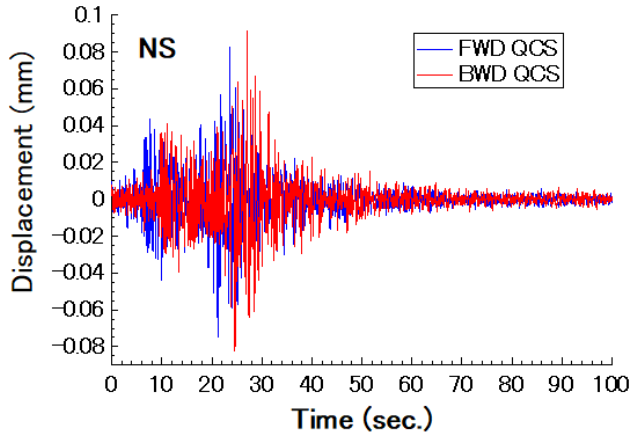

Figure 4. Gap displacements measured by the gap sensors during an earthquake that occurred on May 22, 2022 measured by the gap sensors

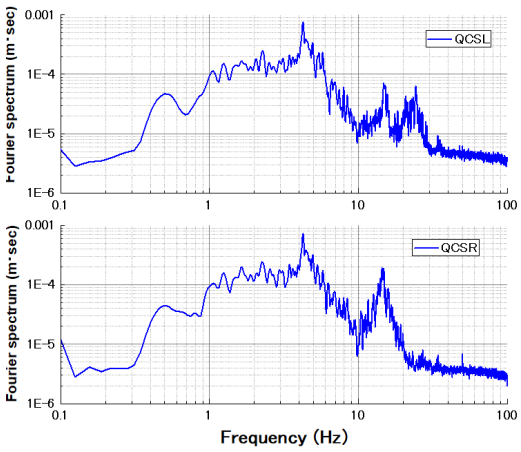

Figure 5. Fourier amplitude spectra of QCS-L (BWD) and QCS-R (FWD) cryostats measured by gap sensors for the earthquake that occurred on May 5, 2022.

The difference between the maximum gap displacements at the two QCSs were very small compared to the individual displacements listed in table 2. Therefore, the gap displacements must have originated from the CDC (i.e., the Belle II detector). The QCSs were unlikely to be the cause, and thus the Belle II detector was the most likely cause. In the next section, the gap displacements calculated by the RSA based on the 3D model of the Belle II detector are compared to the measurements.

4. Verification of the RSA results

4.1 The ground motion at ground level

First, for comparison between the RSA calculations and the measurements, the input ground motion for the RSA was taken from the National Research Institute for Earth Science and Disaster Resilience (NIED), which is located 3 km from KEK in the same neighbourhood [7].

Table 3. Maximum displacement recorded by the measurements ("Meas."), which were the average of the BWD and FWD values in Table 2 and the RSA with the ground motion at the ground level.

Date in 2022	Intensity (I)	RSA (mm)	Meas. (mm)	Difference (mm)
Apr. 19	2.5	0.52	0.3	0.22
May 5	2.4	0.40	0.10	0.30
May 8	0.8	0.05	0.02	0.03
May 22	2.4	0.12	0.10	0.02

As listed in Table 3, the calculations were not perfectly in agreement with the measurements. The major reason for this was that the input ground motion was applied to the ground level, whereas the foundation of the Belle II detector is on a floor 16 m below ground (GL-16m).

4.2 Ground motion at the underground level

After the installation of the acceleration sensors, RSA calculations were also carried out on the Belle II detector 3D model (Belle II-top) using the ANSYS software package, with the ground motion of the GL-16m as the input ground motion.

Table 4. Maximum displacements recorded by the measurements ("Meas.") which were the averages of the values measured at the QCSs, and the RSA results assuming the ground motion at the GL-16m.

Date in 2022	Intensity (I)	RSA (mm)	Meas. (mm)	Difference (mm)
May 29	2.5	0.16	0.17	-0.01
Sep. 9	1.7	0.09	0.06	0.03
Sep. 30	2.1	0.10	0.10	0.00
Nov. 9	2.8	0.17	0.20	-0.03
Nov. 14	2.3	0.17	0.19	-0.02

Table 4 shows the comparison between the RSA calculations and the measurements for this case. For the underground data, the RSA calculations were in good agreement with the measurements. The comparison between RSA the calculations and the measurements in the NS direction for the earthquake that occurred on November 9, 2022, is shown in figure 6.

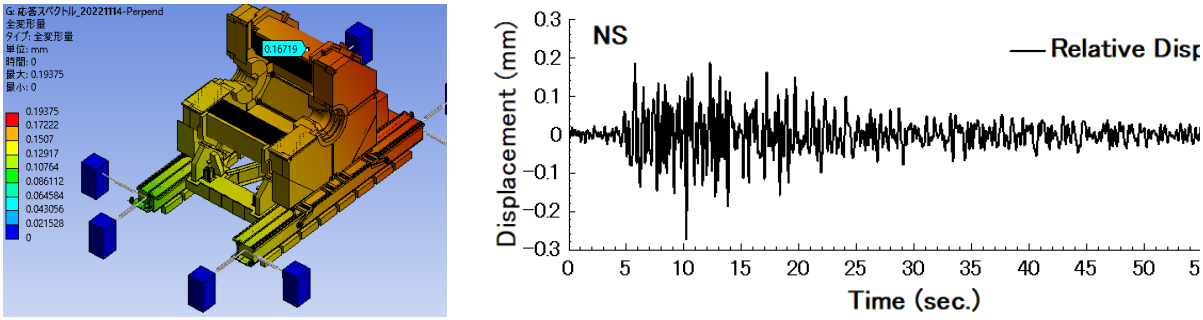

Figure 6. Left panel: maximum displacement for Belle II-top in the NS direction as estimated by the RSA calculations by the ANSYS. Right panel: the displacement measurements for the earthquake that occurred on November. 9, 2022.

5. Measurement of the seismic characteristics on the floor of the Belle II detector

As already mentioned, the Belle II detector rests on a floor 16 m below the ground level. Accordingly, the seismic characteristics measured on that floor were compared to those measured on the ground level. The acceleration histories measured for both the ground level (GL) and the underground level (GL-16m) are shown in the plots in the left column of figure 7. The acceleration values for the underground level in the horizontal (NS and EW) directions were smaller than those for the ground level. However, the acceleration histories in the vertical (UD) direction were almost identical. Converting the acceleration histories to the frequency domain resulted in the acceleration response spectra shown in the right column in figure 7. Seismic waves generally become increasingly damped as measurements are taken further underground. However, the response spectra in the horizontal (NS and EW) directions indicate that they were almost the same for frequencies below 2 Hz. For frequencies above this value, the response spectra for the ground level increased until they reach 10 Hz, while the spectra at the underground level were relatively damped between 2 and 10 Hz. However, the response spectrum in the vertical direction (UD) was not as damped for the underground level.

These observations suggest that detectors or any building with a low natural frequency must be carefully designed, even if they are located underground. In particular, relatively large structures should be designed to optimize their natural frequencies in order to mitigate potential earthquake damage.

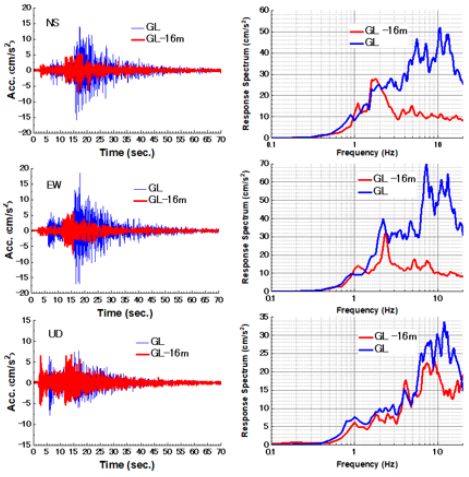

Figure 7. Acceleration histories (left column) and acceleration response spectra (right column) for the ground level (GL) and underground level for the earthquake that occurred on May 29, 2022

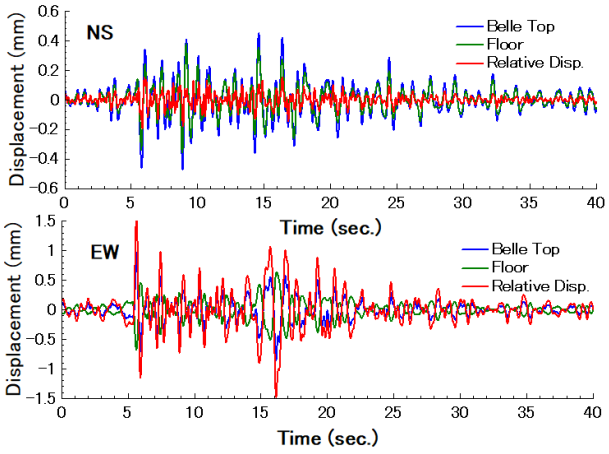

Figure 8. Horizontal displacement measured for the earthquake that occurred on November 9th, 2022

6. Measurement of the relative displacement between the belle ii detector and the floor

The relative displacement between the Belle II detector (Belle II-top) and the underground level (GL-16m) was measured with high-precision acceleration sensors at the start of a long shutdown period for the SuperKEKB accelerator (i.e., at the end of June 2022), during which the detector solenoid was not excited.

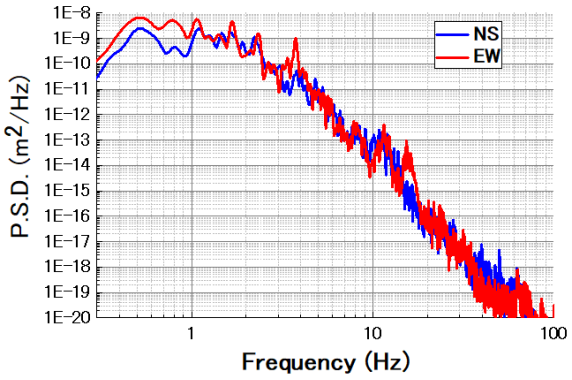

Figure 9. Power spectrum densities (PSDs) of the relative displacements in the NS and EW directions for the earthquake that occurred on November 9, 2022.

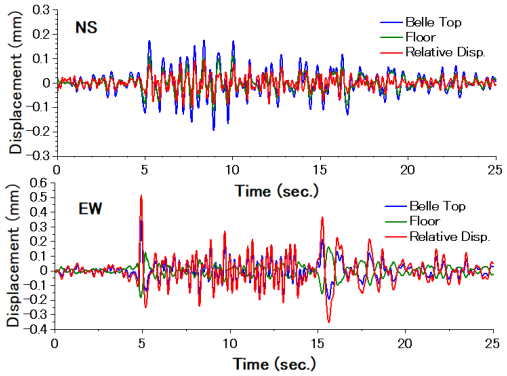

Figure 10. Horizontal displacements measured in the same way as those shown in Figure 8 for the earthquake that occurred on September 30, 2022.

Figure 8 shows typical measurements of the displacement histories for Belle II-top (blue lines) and GL-16m (green lines) in the horizontal directions for the earthquake that occurred on November 9, 2022, which had an intensity of 2.8. The differences between the displacements are shown as the relative displacements (red lines). In the lateral (NS) direction (perpendicular to the beam axis), the displacements at both Belle II-top and GL-16m seem to be in the same phase, as the relative displacements were smaller than the individual displacements. However, in the longitudinal (EW) direction (along the beam axis), the relative phase angle between the Belle II-top and GL-16m displacements reached up to 180 degrees.

The maximum relative displacements in the NS and EW directions were 0.2 mm and 1.5 mm, respectively. To examine this phase behaviour in detail, a fast Fourier transform (FFT) was performed. figure 9 shows the power spectrum densities (PSDs) of the relative displacements in the NS and EW directions, as determined by the FFT analysis. In the NS direction (blue line), no prominent resonant peak was observed. However, there was an obvious resonant peak at 3.5 Hz in the EW direction (red line), which corresponds to the first mode of the resonant frequency of the Belle II detector. This 3.5 Hz resonance has also been observed for other earthquakes.

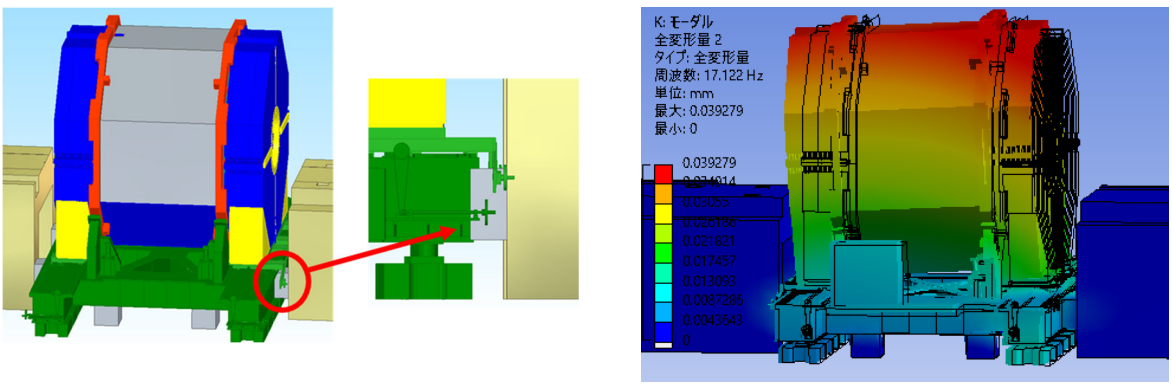

Figure 11. Idea for reinforcement against eartquakes.

Another example is shown in figure 10. It shows the horizontal displacements measured in the same way as those shown in figure 8 for the earthquake that occurred on September 30, 2022, which had an intensity of 2.1. As in figure 8, the relative displacements in the EW direction were larger than the individual ones, and the relative displacements in the NS direction were smaller than the individual ones. The maximum displacements for the EW and NS directions were 0.5 mm and 0.1 mm, respectively. The reason for the phase misalignment phenomenon manifesting only in the EW direction is currently being investigated.

The acceleration caused by an earthquake can be estimated according to $a=0.34\times10^{I/2}$ around the period of 0.3 s, where I am the earthquake intensity defined by the JMA [8]. An earthquake of intensity 4 exerts an acceleration four times that of the earthquake that occurred on November 9, 2022, which had an intensity of 2.8 and caused a maximum relative displacement of 1.5 mm. Using the latter earthquake as a reference, earthquakes with an intensity of 4 can cause a relative displacement in the EW direction of 6 mm, as the displacement is proportional to the acceleration. This exceeds the maximum acceptable displacement of the beam pipe bellows that connect the beam pipe in the QCS, which is rigidly supported at the accelerator tunnel.

One idea proposed for a countermeasure was a square pipe of size 50 × 900 × 800 mm^3 (thickness, height, and width, respectively) that could be connected between the Belle II stand and the bridge for the accelerator at each corner, as shown in Figure 11. A modal analysis indicated that the natural frequency can be increased from 3.5 Hz to 17 Hz. Because the stiffness is proportional to the square of the frequency, the stiffness of this configuration would be 24 times higher, which would allow the deformation to remain within the acceptable tolerance.

7. Conclusion

In this study, the cause of earthquake-induced QCS quench triggers in the Belle II detector was experimentally investigated using gap sensors and high-precision acceleration sensors. The cause of the QCS power shutdown was discovered to be due to the movement of the Belle II detector, and not the QCSs themselves. The RSA results of the Belle II detector model were in good agreement with the ground motion measured at the underground level (GL-16m). For the earthquake characteristics, we found that the acceleration response spectra at the ground and GL-16m levels were almost the same for frequencies below 2 Hz. This is an important factor to consider in the design of soft or large structures, even those constructed underground as their natural frequencies are low, to minimize earthquake damage. The displacements at Belle II-top and GL-16m were measured with high-precision acceleration sensors. The relative displacements were larger than the individual displacements only in the EW direction, where there was a prominent resonance at 3.5 Hz, which is the natural frequency of the Belle II detector when the detector solenoid is not excited. This means that this phenomenon can damage the beam pipe bellows or cause interference in the sub-detectors due to the tolerance disappearing when a strong earthquake occurs. Fortunately, an earthquake with an intensity of 4 or higher has not occurred since we set up the sensors during the long shutdown period of the SuperKEKB accelerator (i.e., the end of June 2022).

We will continue these investigations into the effects of earthquakes on the Belle II detector. In future work, we will develop additional countermeasure ideas to further protect the detector from strong earthquakes.

8. References

[1] N Ohuchi, et al., “SuperKEKB beam final focus superconducting magnet system”, NIM-A, 1021 (2022) 165930.
[2] K Akai et al., “Construction Status of SuperKEKB,” WEOCA01, IPAC’14, Dresden, June 2014; http://www.JACoW.org
[3] X Wang et al., “Design and Performance Test of a Superconducting Compensation Solenoid for SuperKEKB,” IEEE Transaction on Applied Superconductivity, Vol. 26, 2016, Art. no. 742886
[4] T Abe et al., “Belle II Technical Design Report,” KEK Report 2010-1 (2010).

[5] H Yamaoka et al., "Analysis of Earthquake Effect for BELLEII Detector and SUPERKEKB accelerator" IWAA 2022, Geneva, October 2022; https://indico.cern.ch/event/1136611/
[6] K Nakamura, KEK, Private communication
[7] National Research Institute for Earth Science and Disaster Resilience (2019), NIED K-NET, KiK-net, National Research Institute for Earth Science and Disaster Resilience, doi:10.17598/NIED.0004
[8] Japan Meteorological Agency 2023, Calculation Method of Instrumental Seismic Intensity, Japan Meteorological Agency, accessed on February 20, 2023, <https://www.data.jma.go.jp/eqev/data/kyoshin/kaisetsu/calc_sindo.html>.

Acknowledgement
I would like to thank Dr. Tauchi at KEK for his useful advice regarding the seismic data analysis. I would also like to express my gratitude to the Belle II group for giving me the opportunity to conduct this study.